

Stability of supersonic boundary layer on permeable surface

S. A. GAPONOV, YU. G. ERMOLAEV, A. D. KOSINOV,
V. I. LYSENKO, N. V. SEMIONOV, B. V. SMORODSKY

Khristianovich Institute of Theoretical and Applied Mechanics SB RAS
Institutskaya 4/1
Novosibirsk, 630090, Russia
e-mail: vl@itam.nsc.ru

IN THE PRESENT STUDY we have performed combined theoretical and experimental investigation of the surface permeability influence on the linear stability of the supersonic flat-plate boundary layer at free-stream Mach number $M = 2$. Good quantitative agreement was obtained between the data calculated by the linear theory of stability and the data obtained in experiments with artificially generated disturbances performed on models with various porous inserts.

Key words: compressible boundary layer, laminar-turbulent transition, hydrodynamic stability, permeability.

Copyright © 2014 by IPPT PAN

1. Introduction

IN SOLVING MANY ENGINEERING PROBLEMS, very often there arises a problem of the control of boundary layer to be exercised so that it simultaneously provides for a desired flow pattern appropriate for these or those particular purposes. The suction of the gas from boundary layer through a permeable surface is one of control methods. Experiments show that by using porous suction one can delay the onset of turbulence in the boundary layer and shift the position of the laminar-turbulent transition in the downstream direction. At subsonic flow velocities, critical Reynolds numbers of about $Re_c = 40 \cdot 10^6$ were experimentally obtained. Nowadays, many theoretical studies are available that attribute the stabilizing action of suction to a reduced thickness of boundary layer and to the formation of a more stable velocity profile.

Thus, both experimental and theoretical data point to a possibility of stabilizing boundary layer by suction. Detailed information on flow stabilization at subsonic and supersonic velocities can be found in the monographs [1, 2] and in many other sources. The majority of theoretical studies of boundary-layer stabilization by suction disregard the properties of permeable surfaces, which may have a profound influence on stability. The influence of the properties of the permeable coating on the stability of subsonic boundary layer was theoretically

examined for the first time by S. A. GAPONOV [3]. In subsequent publications, the author advanced an impedance relation for velocity perturbations and pressure on a permeable surface taking into consideration the effects of gas compressibility. This relation was used to study both subsonic [3] and low Mach number supersonic flows [4].

The cited papers dealt only with the theory, while the experimental studies of the problem of interest were absent in the literature throughout the world for a long time; the latter case can be best explained, first of all, by the absence of a high-quality material for permeable coating. In turn, the lack of experiments was a suppressing factor for the development of a theoretical model. However, presently the situation has changed. Recently, experiments on stability of hypersonic [5–8] and supersonic [9] boundary-layer have been performed. The results of those experiments are in a satisfactory agreement with calculations [10–12] based on the approach proposed in [3, 4].

In our earlier paper [9] it was found that increase of pore radius moves upstream the location of transition on porous surface. Thus, it was shown that at supersonic speeds application of permeable coating accelerates the transition in contrast to hypersonic boundary layer where porosity delays the transition.

This difference is related to the fact that the transition at supersonic velocities is defined by the first instability mode whereas at hypersonic velocities an important role in the transition is played by the second instability mode. An investigation of the first mode is more complicated because instability with respect to this mode is determined by oblique (three-dimensional) waves, whereas instability related to the second mode is determined by two-dimensional waves.

This paper presents theoretical and experimental study of the porous coating influence on the stability of supersonic boundary layer at Mach number $M = 2$. For the first time, the development of disturbances artificially introduced in the boundary layer, at this Mach number, has been experimentally examined. A direct comparison of measured and computed amplification curves and spatial amplification rates is given.

2. Experimental setup

The experiments were carried out in the T-325 wind tunnel of ITAM, SB RAS [13] at free-stream Mach number $M_\infty = 2$, stagnation temperature $T_0 \approx 295$ K, and unit Reynolds number $Re_{1\infty} \approx 5 \cdot 10^6 \text{ m}^{-1}$. Since this is a continuously running tunnel, the thermal boundary condition at the model surface during typical experimental run (~ 40 minutes) was an insulated wall. That means that the wall temperature was equal to the recovery temperature and, for selected M_∞ and T_0 , it was close to the ambient temperature: $T_{\text{wall}} \approx 273$ K.

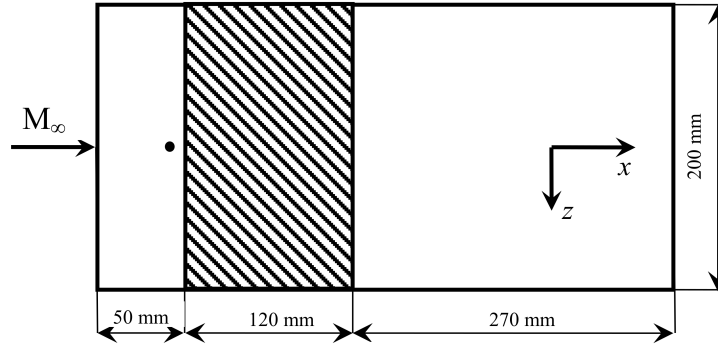


FIG. 1. Schematic of the experimental flat-plate model – plan view. The porous insert is shown as a shaded region. The position of the disturbance generator is shown by the small circle $x_{\text{source}} = 37$ mm.

The model was a flat plate made of stainless steel, 440 mm long, 10 mm thick, and 200 mm wide, with a skew nose cut at angle 14° and with a sharp leading-edge (bluntness radius was not more than 0.05 mm). A schematic of the model is given in Fig. 1. The origin of the streamwise coordinate x to be used in the present study (in the free-stream direction) is at the leading edge of the model. Over the working-surface segment 50 to 170 mm throughout the whole width of the plate the plate was provided with a 4.3 mm deep slot used for fixation of replaceable insert-plates of different porosities and pore sizes. Three inserts have been used: a solid impermeable stainless-steel plate (insert 1); a 39%-porosity plate manufactured of PNS-8 porous stainless steel with $10 \mu\text{m}$ filtration purity (analogues to the pore diameter – insert 2) and a 32%-porosity plate prepared from TPP-5-MP porous titanium of $40 \mu\text{m}$ filtration purity (insert 3). Inserts 2 and 3 were prepared from a material commercially available from the Metallurgical Plant located at Vyksa, Russian Federation. Parameters of the porous inserts used in measurements are also collected in Table 1.

Table 1.

Insert	Porosity n , %	Manufacturer's filtration purity $2r$, μm	LST $2r$, μm
1	0	0	0
2	39	10	15
3	32	40	60

It should be mentioned that we have used inserts with finite (small) thickness coating, made of penetrable porous material. However, below the porous insert plate there was the stainless steel impermeable substrate. That means there was

no mean transpiration flow through the inserts. Only the fluctuation pressure fields, developing in the boundary layer as a result of instability, were penetrating the pores and underwent the viscous damping within porous channels. Therefore in our measurements we have investigated only the influence of porosity on the boundary layer instability alone, with zero mean flow through the surface under study.

The plate under the study was fixed rigidly to the sidewalls of the test section of the wind tunnel at zero angle of attack. Artificial disturbances have been introduced in the boundary layer over the model by means of point glow discharge disturbance generator [14]. Investigation of controlled disturbance evolution in the boundary layer has been performed by a constant-resistance hot-wire anemometer operated with a single-wire sensor made of 10 μm diameter tungsten wire of length 1.5 mm. The overheat ratio of the sensor was 0.8; therefore, it could be assumed that the probe was sensitive predominantly to the mass-flux fluctuations. Measurements of the downstream disturbance amplification have been performed in the vicinity of a maximal fluctuation layer, at $E = \text{const}$ (where E is the mean diagonal voltage across the hot-wire bridge), i.e., along the line of a constant value of the mass flux. Disturbance measurements have been performed around the line ($y = 0, z = 0$) corresponding to the model centerline, at $|z| < 15$ mm, that was far enough from the test section's sidewalls (located at $|z| = 100$ mm), to reduce a possible parasitic influence of sidewalls.

The fluctuation and mean flow quantities were measured by means of an automated data acquisition system described in more detail in [15, 16]. The fluctuation voltage from the hot-wire anemometer was fed in a PC by the analog-to-digital converter with sampling rate of 750 kHz. A total of 65 536 points were measured. The average anemometer voltage was measured by an Agilent 34401A voltmeter; this voltage was subsequently fed into the PC through the serial port. Indications of time-mean and fluctuation flow properties have been taken in several streamwise measurement stations. The amplitude-frequency spectrum $A(f, x)$ has been computed by averaging the measured power spectra.

3. Linear stability theory

Calculations on the basis of linear stability theory (LST) have been performed with the assumption of a perfect gas with constant values of specific heat ratio $\gamma = 1.4$ and Prandtl number $\text{Pr} = 0.72$. It was assumed that viscosity μ is a function of the temperature only according to the Sutherland relation. Within the framework of the linear stability problem, we represent the flow field in the compressible boundary layer as combination of a time-mean flow and a low-amplitude perturbation. The main flow is considered in the local-parallel approximation [17]. The equations for disturbances result from linearization of

equations of motion for a viscous heat-conducting compressible gas (Navier–Stokes, continuity and energy equations). We represent the solution of the problem as a set of harmonic waves

$$\mathbf{q} = A(x)\boldsymbol{\Phi}(y) \exp\left(i \int_{x_0}^x \alpha(x') dx' + i\beta z - i\omega t\right),$$

where (x, y, z) are streamwise, normal-to-the surface, and spanwise coordinates, the disturbance wave vector $\mathbf{k} = (\alpha, \beta)$ is composed of the streamwise α and spanwise β wavenumbers, $\omega = 2\pi f$, f is the frequency. All quantities were taken nondimensional in the standard way, that means with respect to the length scale $\delta = \sqrt{U_e \rho_e x / \mu_e}$ of the Blasius laminar boundary layer, mean velocity U_e and values of pressure, density, temperature and viscosity taken at the outer edge of the boundary layer: P_e, ρ_e, T_e, μ_e . Then, for the sought vector $\boldsymbol{\Phi} = (u, u', v, p, \theta, \theta', w, w')^T$, composed of perturbations of the three components of velocity (u, v, w) , pressure p and temperature θ , and their derivatives with respect to y , we obtain a system of linear ordinary differential equations

$$(3.1) \quad \frac{d\boldsymbol{\Phi}}{dy} = L(U, T)\boldsymbol{\Phi}.$$

The non-zero elements of the linear Lees–Lin operator L are given in [18]; they depend on the properties of the mean flow (through the surface-normal profiles of mean velocity and temperature $(U(y), T(y))$ and on the parameters of the wave such as frequency and wavenumbers. System (3.1) has to be solved under the following boundary conditions. At the boundary layer outer edge we have

$$(3.2) \quad |\boldsymbol{\Phi}| \rightarrow 0, \quad (y \rightarrow \infty).$$

According to [3, 4], the conditions on the permeable surface are

$$(3.3) \quad u(0) = w(0) = \theta(0) = 0, \quad v(0) = Kp(0),$$

where the complex parameter K is the acoustic admittance of the porous coating.

To investigate the spatial stability, we assume that the frequency and the spanwise wavenumber to be real quantities, while the streamwise wavenumber α is a complex number. Then, $\alpha = \alpha_r + i\alpha_i$ can be found as an eigenvalue of boundary-value problem (3.1)–(3.3), while the components of $\boldsymbol{\Phi}$ will be obtained as corresponding eigenfunctions of the problem. Here, the waves with $-\alpha_i > 0$ refer to unstable disturbances growing in the downstream direction, while the waves with $-\alpha_i \leq 0$ are stable decaying with x .

The magnitude and the phase of K depend on the properties of the porous coating, characteristics of the boundary layer, such as the boundary layer thickness and the Mach number at the outer edge of the boundary layer, and on the

characteristics of the wave propagating in the boundary layer. In the present study, we examine stability of boundary layer on a flat plate covered by a porous layer of finite thickness h^* (in this paragraph, the asterisk in the superscript denotes a dimensional quantity, whereas all variables without asterisk are assumed to be nondimensionalized using the corresponding parameters). We consider a porous coating in the form of a thin flat plate with cylindrical pores uniformly covering surface of the model, having a constant radius r^* and oriented normal to the surface. The pore radius and the pore-to-pore distance s^* are assumed to be much smaller in comparison to the boundary layer thickness and therefore smaller than typical instability wave length.

For determination of the admittance K in the case of a compressible gas the author of [3] used the theory of sound propagation in a long narrow channels, assuming also $r^* \ll h^*$. In such a case, the propagation of an acoustic wave is governed by the propagation constant Λ and by the impedance Z_0 :

$$(3.4) \quad \Lambda = \sqrt{Z_1 Y_1}, \quad Z_0 = \sqrt{Z_1 / Y_1},$$

$$Z_1 = \frac{i\omega}{T_w} \frac{J_0(k)}{J_2(k)}, \quad Y_1 = -i\omega M_e^2 \left[\gamma + (\gamma - 1) \frac{J_2(k\sqrt{\text{Pr}})}{J_0(k\sqrt{\text{Pr}})} \right],$$

$$(3.5) \quad k = r \sqrt{\frac{i\omega \rho_w}{\mu_w} \text{Re}},$$

where M_e is the Mach number at the boundary layer's outer edge, ρ is the gas density, $r = r^*/\delta$ is the pore radius nondimensionalized by the Blasius length scale δ , J_0, J_2 are the Bessel functions of the corresponding order and the subscript w denotes the value of a quantity at the wall. For blind pores, closed at their bottom (at $y^* = -h^*$) by a solid wall, the admittance K can be represented as

$$(3.6) \quad K = \frac{n}{Z_0} \tanh(\Lambda h),$$

where n is the coefficient of surface porosity that defines the surface area fraction occupied by the pores. One can see that the magnitude of the acoustic admittance K (3.6), which will determine the stability properties of the boundary layer over the porous layer, is directly proportional to the porosity n and depends also on the pore radius r (3.5). In our measurements we have used porous inserts with close values of porosity but with quite different pore sizes, see Table 1. If the porous layer is sufficiently thick ($\Lambda h \gg 1$) (which is often the case), then we have

$$(3.7) \quad K = -\frac{n}{Z_0}.$$

Derivation of relations (3.3)–(3.7) is described in more detail in [3, 4, 9].

The stability calculations have been performed numerically by integrating the boundary-value problem for the eigenvalues of (3.1)-(3.3) with regard to relations (3.6) or (3.7) using the orthonormalization method [2]. Some results of computations of the stability of supersonic boundary layer on a porous surface at free-stream Mach number $M_\infty = 2$ have been described earlier in [19], while in [9] a comparison with experiments performed with natural disturbances has been presented.

4. Results

Figure 2 shows LST data of the influence of the pore radius on the growth rates of the unstable fluctuations in the supersonic $M = 2$ boundary layer. Normalized spatial amplification rates $-\alpha_i \delta / \text{Re}_1 \cdot 10^6$ of disturbances with the reduced frequency $F = 50 \cdot 10^{-6}$, at Reynolds number based on the Blasius length scale $R = U_e \rho_e \delta / \mu_e = 600$, are depicted as a function of wave vector orientation angle $\chi = \arctan(\beta/\alpha)$ for various values of nondimensional pore radii $0 \leq r/\delta \leq 1$. Increase of r leads to monotonous enlargement of wave growth rates for all angles $0 \leq \chi < 75^\circ$. In addition angle χ_{\max} corresponding to the maximal growth rate $-\alpha_{i,\max} = \max_\chi(-\alpha_i)$ is shifted from $\chi_{\max} \approx 58^\circ$ at $r = 0$ to $\chi_{\max} \approx 42^\circ$ at $r = 1$. However the strongest influence of the porous coating on the amplification of perturbations occurs at small angles $0 \leq \chi \leq 20^\circ$, whereas waves with higher inclination angles $\chi \geq 65^\circ$ are influenced by porosity much weaker. Thus, an increase of the pore radius causes destabilization of the su-

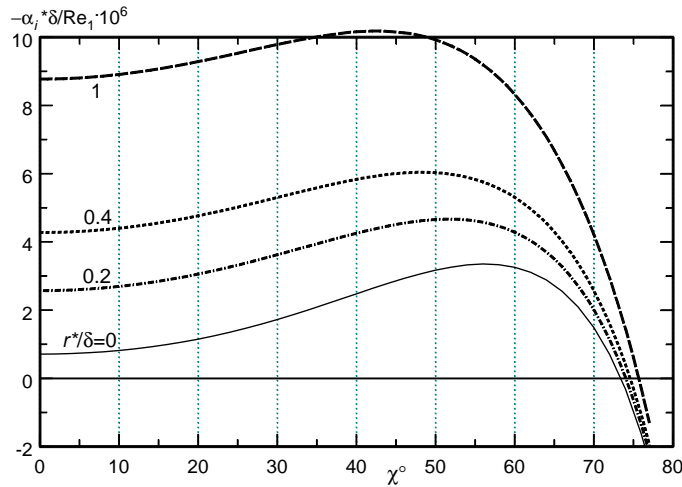


FIG. 2. Normalized disturbance growth rates $-\alpha_i \delta / \text{Re}_1 \cdot 10^6$ versus wave vector orientation angle χ for various non-dimensional pore radii $0 \leq r/\delta \leq 1$; $F = 50 \cdot 10^{-6}$, $R = 600$.

personic boundary layer. In the experiments on stability of hypersonic ($M \approx 6$) boundary layer [5–8] the influence of permeable coating on the amplification of two-dimensional (2D, $\chi = 0^\circ$) fluctuations has only been investigated. So the subject of the present paper is the direct quantitative comparison of LST computations and experimental data for disturbances with $\chi \geq 0^\circ$.

The stability diagram of the model boundary layer with the impermeable insert 1 for conditions of actual experiment is presented in Fig. 3 by contour lines of dimensional spatial amplification rates for 2D-waves on the plane streamwise coordinate x –frequency f : $-\alpha_i = -\alpha_i(x, f)$. Color-flooded area corresponds to the region of the linear instability where fluctuations are amplifying downstream. Position of the inserts is sketched by the grey strip starting at $x = 50$ mm, while the location of the disturbance generator is depicted by a small square “Source”. Disturbance amplitude measurements have been performed in the boundary layer above the inserts by a hot wire probe in seven streamwise stations ($x = 50, 65, 80, 95, 110, 125, 140$ mm) shown in Fig. 3 by red vertical columns. The initial disturbance β -spectrum on the excitation frequency has been measured at $x = 50$ mm, still on the solid surface. The computed stability diagram gives an idea about an unstable frequency range. In particular, the most amplifying frequency in the middle of the measurement domain (at $x = 95$ mm) are 2D disturbances with $f \approx 14$ kHz (horizontal red line). Therefore in our measurements this frequency has been chosen as a frequency of artificial disturbance generation.

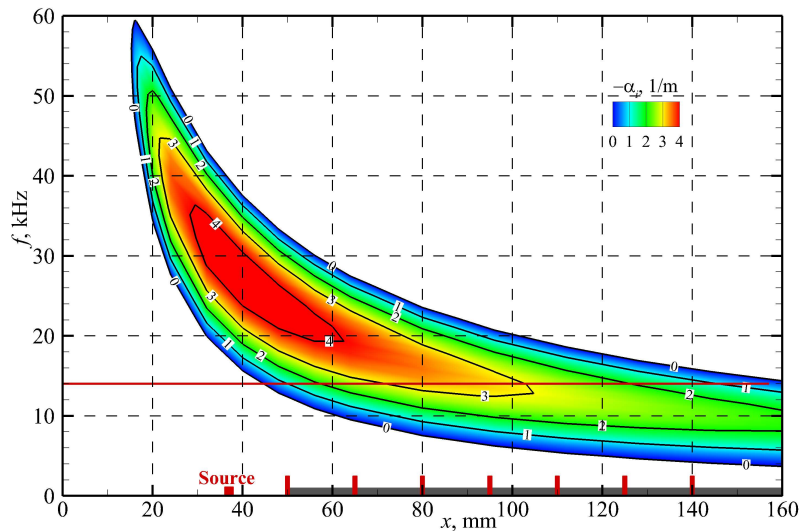


FIG. 3. Stability diagram for the insert 1: dimensional (m^{-1}) spatial amplification rate contours $-\alpha_i = -\alpha_i(x, f)$, $\chi = 0^\circ$.

The stability diagram for three-dimensional (3D) disturbances computed for the central measurement station ($x = 95$ mm) is shown in Fig. 4. One can see that under conditions of measurements with the impermeable insert 1 according to the LST the most unstable 3D perturbations are waves with $f \approx 15$ kHz and $\chi \approx 60^\circ$ (red color region). Amplification rate of such disturbances is about five times larger in comparison to 2D perturbations.

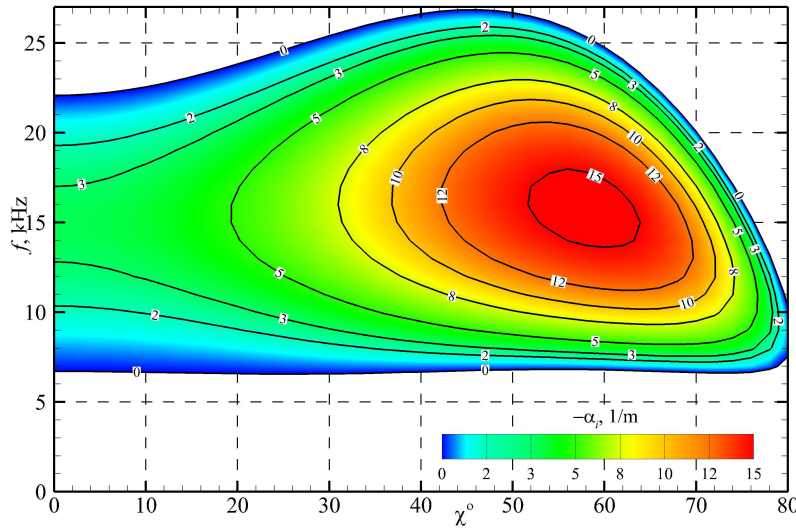


FIG. 4. Spatial amplification rate contours for insert 1: $-\alpha_i = -\alpha_i(\chi, f)$ [m^{-1}], $x = 95$ mm.

Figure 5 demonstrate β -spectra measured on the excitation frequency $f = 14$ kHz in experiments with inserts 1, 2, 3, respectively. The normalized root-mean-square fluctuation amplitudes $A_{f\beta}$ at measurement stations are shown versus the dimensional spanwise wavenumber β [rad/mm]. One can see that in all three experiments with inserts 1–3 the most amplifying in the downstream direction are disturbances with $\beta = 0.5 \div 0.6$ rad/mm.

In addition one can see from Fig. 5a that for impermeable insert 1 perturbations with $\beta = +0.65$ rad/mm are amplified in seven times on a distance of $50 \leq x \leq 140$ mm while disturbances with $\beta = -0.65$ rad/mm have increased five and a half times. Thus, a certain asymmetry of the disturbance field is developing at most downstream measurement station. In measurements with small-pore insert 2 (Fig. 5b) not only 3D fluctuations with $|\beta| \approx 0.5$ rad/mm are amplified but there is also an anomalous growth of 2D perturbations $|\beta| < 0.2$ rad/mm. In experiments with the large-pore insert 3 (Fig. 5c) an anomalous growth of 2D fluctuations is also visible but it is weaker.

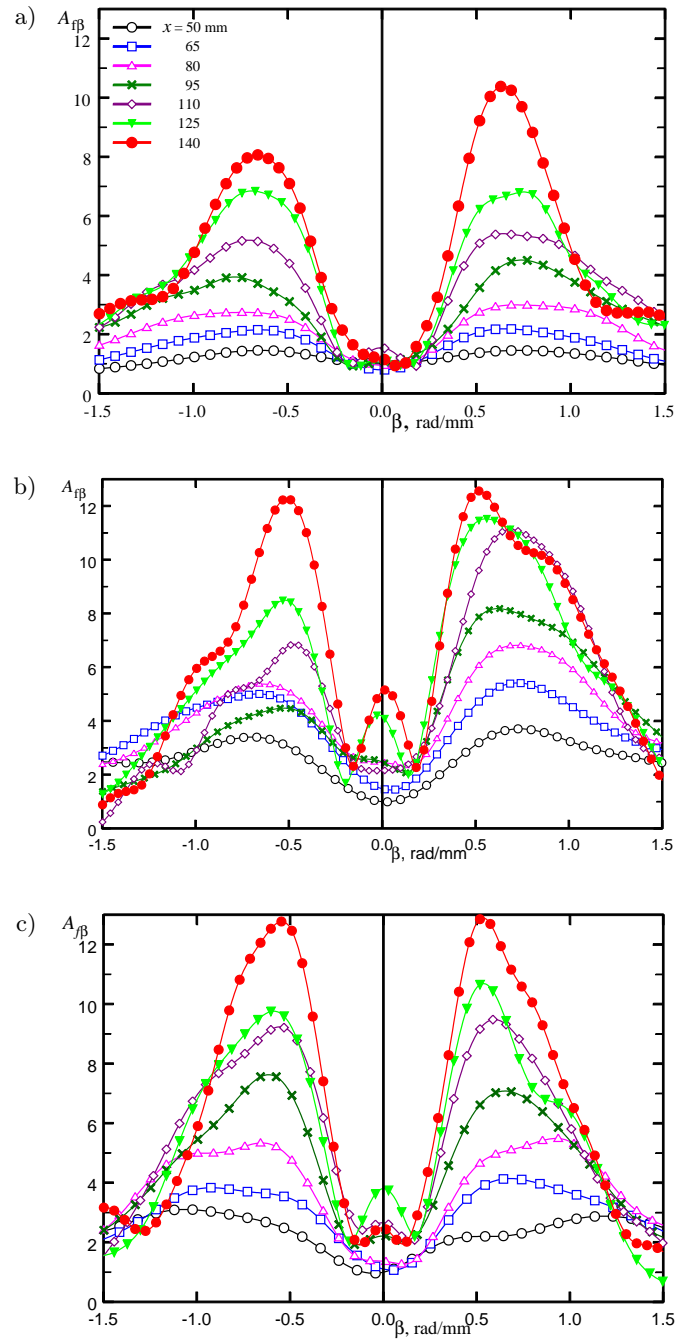


FIG. 5. Measured disturbance spectra: normalized rms fluctuation amplitudes $A_{f\beta}$ versus spanwise wavenumber β at various streamwise stations $50 \leq x \leq 140$ mm for inserts 1–3 (a–c, respectively), $f = 14$ kHz.

Figure 6 presents an example of comparison of the measured and computed disturbance amplification curves for insert 3 at $f = 14$ kHz and $\beta = \pm 0.6$ rad/mm (closed and open symbols respectively). Computations have been performed not only for the nominal value of the pore diameter $2r = 40$ μm given by the producer of the porous material but also for some other values. One can see that the best agreement of the computed amplification curve with measurements can be obtained with the value of $2r^* = 60$ μm that is 50% larger than the filtration purity given by the producer. Similar computations have been performed for various values of β and also for insert 2. The conclusion made from such a comparison is that for both porous inserts with small and large pores the diameter of pores used in LST computations should be taken 50% higher than the value given by the producer. Only then, it is possible to obtain good overall agreement of theory and measurements for disturbance amplification curves. The values of pore diameters used in LST computations are shown in the last column of the Table 1.

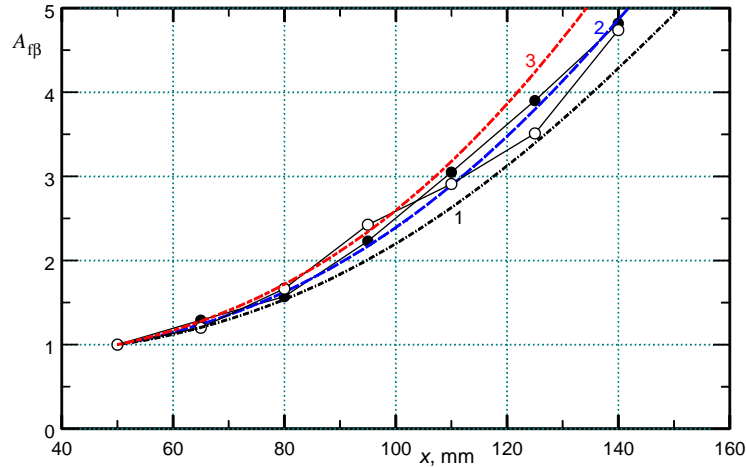


FIG. 6. Normalized disturbance amplification curves for insert 3: $f = 14$ kHz, $\beta^* = \pm 0.6$ rad/mm. Comparison of experiment (symbols) and LST (dashed lines): $2r^* = 40, 60, 80$ μm (curves 1–3 respectively).

Figure 7 shows direct comparison of the measured and computed local spatial amplification rates $-\alpha_i = -\alpha_i(\beta)$ for the middle of the measurement area $x = 95$ mm. Experimental growth rates have been determined by means of polynomial regression of the measured data for growth curves $\ln A(x)$ of disturbances with different β . The growth rate was then determined by the formula $-\alpha_i = \partial \ln A(x) / \partial x$. Dimensional values of the amplification rate are shown in Fig. 7 versus the spanwise wavenumber. LST computations have been performed for various values of the pore diameter $2r^*$ which was 50% higher the value given

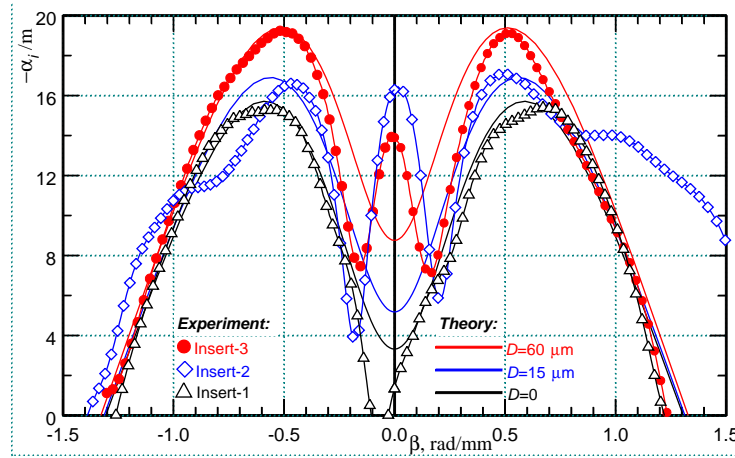


FIG. 7. Disturbance spatial amplification rates $-\alpha_i$ versus spanwise wavenumber β for inserts 1–3; $x = 95$ mm. Comparison of LST (solid lines) and measurements (symbols).

by the producer. One can see a good agreement of computed (solid lines) and experimental (symbols) amplification rates at $|\beta| \geq 0.25$. Increase of the pore diameter leads to the increase of the growth rates for all values of β , but this influence is, theoretically, stronger at $\beta \approx 0$. The location of maximal growth rates $-\alpha_{i,\max} = \max_{\beta}[-\alpha_i(\beta)]$ computed for conditions of measurements is shifted from $|\beta| \approx 0.6$ at $r = 0$ (insert 1) to $|\beta| \approx 0.5$ at $2r \approx 40 \mu\text{m}$ (insert 3). One can see that positions of maximal growth rates correlate well for inserts 1 and 3. For insert 2 with small pores the agreement of theory with measurement is not so good. The possible explanation of this discrepancy is an uncontrolled nonzero angle of attack of the model. The magnitude of the maximal experimental increments $-\alpha_{i,\max}$ agrees also well with LST data. The disagreement is observed for small values of $|\beta| < 0.2$. In the experiment a strong anomalous growth at β close to zero occurs. The reason for this discrepancy is a beginning of nonlinear processes in the boundary layer. Absolute fluctuation level for inserts 2 and 3 is higher in comparison to insert 1. Computation of the local growth rates also shows that the best agreement with measurements can be obtained with the pore sizes 50% larger the values of the filtration purity of the porous material given by the producer.

5. Conclusions

Combined theoretical and experimental investigation of the porous coating influence on the stability of flat plate supersonic boundary layer at $M = 2$ has been performed. Good quantitative agreement of LST computations with ex-

periments performed on models with various porous inserts has been achieved. Experimental data have been obtained by the use of artificial disturbance glow discharge-based generator. Theoretical and experimental integral amplification curves and local spatial amplification rates correlate well. Since samples of porous material available for our measurements have almost the same porosity but quite different pore sizes (Table 1) the conclusion can be made that, similar to the case of the natural disturbance development, the increase of the pore diameter leads to the boundary layer destabilization that accelerates the laminar-turbulent transition. The results of the performed theoretical and experimental investigations qualitatively indicate that at supersonic speeds the stabilizing influence of suction on the boundary layer stability and transition can be jeopardized or overcome by the destabilizing influence of permeable surface on the development of boundary layer eigen unstable fluctuations.

Acknowledgment

This paper was supported by Russian Foundation for Basic Research (Project 12-01-00158-a).

References

1. A.V. BOIKO, G.R. GREK, A.V. DOVGAL, V.V. KOZLOV, *Physical Mechanisms of Transition to Turbulence in Open Flows*, Regular and Chaotic Dynamics, Moscow, 2006.
2. S.A. GAPONOV, A.A. MASLOV, *Development of Disturbances in Compressible Flows*, Nauka, Novosibirsk, 1980.
3. S.A. GAPONOV, *Effect of gas compressibility on the stability of a boundary layer above a permeable surface at subsonic velocities*, J. Appl. Mech. Tech. Phys., **16**, 1, 95–98, 1975.
4. S.A. GAPONOV, *Stability of the supersonic boundary layer on a permeable surface with heat transfer*, Fluid Dynamics, **12**, 1, 33–38, 1977.
5. V.M. FOMIN, A.V. FEDOROV, A.N. SHIPLYUK, A.A. MASLOV, E.V. BUROV, N.D. MALMUTH, *Stabilization of a hypersonic boundary layer by ultrasound absorbing coatings*, Doklady Physics, **47**, 5, 401–404, 2002.
6. V.M. FOMIN, A.V. FEDOROV, V.F. KOZLOV, A.N. SHIPLYUK, A.A. MASLOV, E.V. BUROV, N.D. MALMUTH, *Stabilization of a hypersonic boundary layer by ultrasound absorbing coatings with a regular microstructure*, Doklady Physics, **49**, 12, 763–767, 2004.
7. N. CHOKANI, D.A. BOUNTIN, A.N. SHIPLYUK, A.A. MASLOV, *Nonlinear aspects of hypersonic boundary layer stability on a porous surface*, AIAA J., **43**, 1, 149–155, 2005.
8. A. RASHEED, H.G. HORNING, A.V. FEDOROV, N.D. MALMUTH, *Experiments on passive hypervelocity boundary-layer control using an ultrasonically absorptive surface*, AIAA J., **40**, 3, 481–489, 2002.

9. S.A. GAPONOV, YU.G. ERMOLAEV, A.D. KOSINOV, V.I. LYSENKO, N.V. SEMIONOV, B.V. SMORODSKY, *Influence of surface porosity on stability and transition of the flat plate supersonic boundary layer*, Thermophysics and Aeromechanics, **17**, 2, 281–290, 2010.
10. A.V. FEDOROV, N.D. MALMUTH, A. RASHEED, H.G. HORNUNG, *Stabilization of hypersonic boundary layers by porous coatings*, AIAA J., **39**, 4, 605–610, 2001.
11. A.V. FEDOROV, A.N. SHIPLYUK, A.A. MASLOV, E.V. BUROV, N.D. MALMUTH, *Stabilization of a hypersonic boundary layer using an ultrasonically absorptive coating*, J. Fluid Mech., **479**, 99–124, 2003.
12. S.A. GAPONOV, N.M. TEREKHOVA, *Linear evolution and interaction of disturbances in the boundary layers on impermeable and porous surfaces in the presence of heat transfer*, Fluid Dynamics, **46**, 412–417, 2011.
13. G.I. BAGAEV, V.A. LEBIGA, V.G. PRIDANOV, V.V. CHERNYKH, *T-325 low-turbulence supersonic wind tunnel*, in: Aerophysical Research, Novosibirsk, ITAM, USSR Acad. Sci., Siberian Branch, 11–13, 1972.
14. A.D. KOSINOV, N.V. SEMIONOV, S.G. SHEVELKOV, *Investigation of supersonic boundary layer stability and transition using controlled disturbances*, Proc. Intern. Conf. Meth. Aerophys. Research. Novosibirsk, Pt. 2, 159–166, 1994.
15. A.D. KOSINOV, N.V. SEMIONOV, YU.G. ERMOLAEV, *Disturbances in the test section of T-325 supersonic wind tunnel*, Preprint No. 6-99, ITAM SB RAS, Novosibirsk, 1999.
16. A.D. KOSINOV, YU.G. ERMOLAEV, N.N. NIKOLAEV, N.V. SEMIONOV, A.I. SEMISYNOV, *On the measurements of the pulsation in supersonic boundary layer by constant temperature hot-wire anemometer*, in: Proc. Int. Conf. on the Methods of Aerophysical Research, Pt. 5, Novosibirsk, 81–86, 2007.
17. W.D. HAYES, R. PROBSTEIN, *Hypersonic Flow Theory*, Academic Press, N.Y., 1959.
18. V.N. ZHIGULEV, A.M. TUMIN, *Turbulence Origin*, Nauka, Novosibirsk, 1987.
19. S.A. GAPONOV, B.V. SMORODSKY, *Linear stability of supersonic boundary layer on porous surface*, in: Recent Advances in Fluid Mechanics and Aerodynamics, Moscow, 68–73, 2009.

Received October 31, 2013; revised April 4, 2014.
